JACS
JOURNAL OF THE AMERICAN CHEMICAL SOCIETY
pubs.acs.org/JACS
Article

Reactivity and Selectivity Controlling Factors in the Pd/Dialkylbiarylphosphine-Catalyzed C−C Cleavage/Cross-Coupling of an N-Fused Bicyclo α-Hydroxy-β-Lactam

Li-Ping Xu, Jose B. Roque, Richmond Sarpong,* and Djamaladdin G. Musaev*

Cite This: J. Am. Chem. Soc. 2020, 142, 21140−21152
Read Online
ACCESS | Metrics & More | Article Recommendations | Supporting Information

ABSTRACT: Density functional theory was employed in order to elucidate the mechanism and factors that lead to the observed regioselectivity in the dialkylbiarylphosphine (Phos)/Pd-catalyzed C−C cleavage/cross-coupling of an *N*-fused bicyclo α-hydroxy-β-lactam, **1**. We have identified that (a) a complex [(**1**)(Cs_2CO_3)]-PdL(PhBr) forms prior to a "*base-mediated oxidative addition*"; (b) Cs-carbonate (rather than a halide) deprotonates the alcohol substrate in the lowest energy pathway en route to Pd-alcoholate formation; (c) reactions using Phos ligands bearing OCF_3 and OCF_2H substituents on the "B"-ring are predicted to be selective toward proximal ring opening of **1**; (d) steric repulsion between the bottom "B"-ring of the Phos ligand and the piperidine moiety of **1** controls the regioselectivity of the C−C cleavage followed by cross-coupling; and (e) the α- vs β-selective functionalization of the piperidine moiety in **1** is influenced by the bulkiness of the R^2-substituent of the coupling partner. These studies will aid in the design of selective functionalizations of the piperidine moiety in **1**.

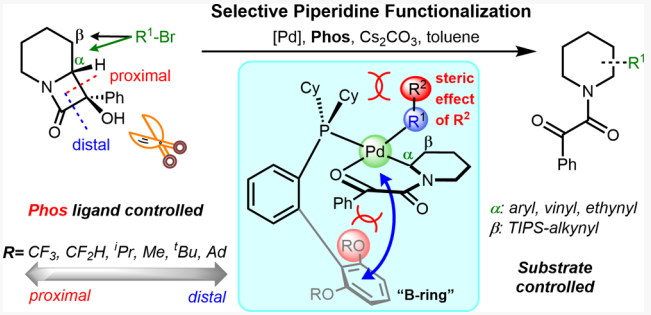

INTRODUCTION

The latest advances in C−H functionalization continue to open new ways for efficient site- and stereoselective synthesis.[1] Many novel complex molecules and fine chemicals sought in the pharmaceutical, agrochemical, and materials industries can now be envisioned from easily accessible precursors on the basis of C−H functionalization strategy.[1] One set of versatile precursors that lend themselves well to C−H functionalization are C(sp^3)-rich alicyclic amines (saturated aza-cycles). Their C−H functionalization, especially of piperidines, has been the subject of a number of pioneering studies. For example, Coldham and Leonori,[2] Knochel and co-workers,[3] and Baudoin and co-workers[4] have independently reported α- or β-arylation of *N*-Boc protected piperidines using lithiation and transmetalation to a Zn species followed by Negishi cross-coupling (Scheme 1, eq 1). Seidel and co-workers have expanded this reactivity paradigm to the α-functionalization of unprotected cyclic amines (Scheme 1, eq 2).[5] Alternatively, Sames and co-workers and Maes and co-workers have reported α-arylation of piperidines with amidine and pyridyl directing groups, respectively (Scheme 1, eq 3).[6,7] Yu and co-workers, Glorius and co-workers, and Gong and co-workers have employed thioamide derivatives as directing groups to achieve the enantioselective α-functionalization of saturated aza-heterocycles (Scheme 1, eq 3; where Y = S).[8]

Despite these significant advances, strategies that rely on deprotonation with a strong base are limited in terms of functional group tolerability, whereas those that employ directing groups can be specific in their applications. Mild methods which achieve controlled site selectivity would facilitate the exploration of novel chemical space through late-stage functionalization. In this context, strategies developed by Sarpong and co-workers,[9] Baudoin and co-workers,[4] and Sanford and co-workers[10] (Scheme 1, eq 4) for the α-, β-, and γ-selective arylation of piperidines (and other saturated aza-cycles) are representative of many emerging approaches toward this goal. For example, Sarpong and co-workers have demonstrated the utility of N-fused bicyclo α-hydroxy-β-lactam, **1** (Scheme 2), generated under mild visible light conditions from phenyl keto amides, for piperidine C−H functionalization by effecting a C−C cleavage/cross-coupling.[9] Specifically, they have identified palladium complexes bearing Buchwald dialkylbiaryl phosphine ligands (Phos)[11] to be important for achieving α- and/or β-selective piperidine arylation, vinylation, and alkynylation in **1** and related azacycles.[9,12]

Received: September 24, 2020
Published: December 8, 2020

https://dx.doi.org/10.1021/jacs.0c10220
J. Am. Chem. Soc. 2020, 142, 21140−21152

Scheme 1. Selected Examples for the C−H Functionalization of Piperidine

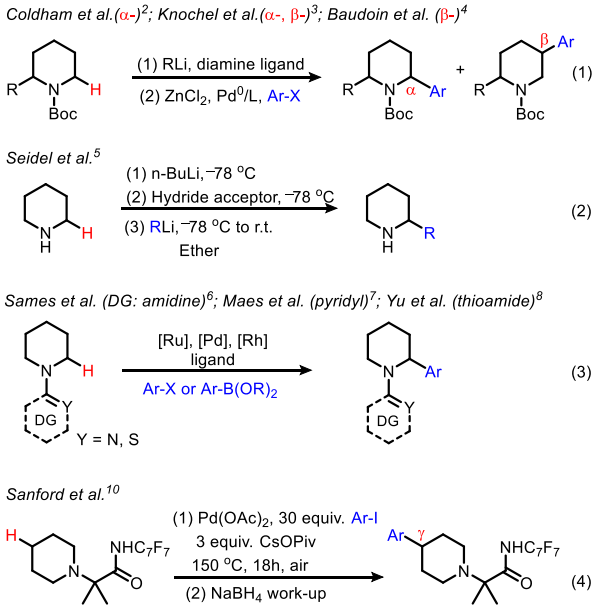

Scheme 2. Selective α- vs β-Functionalization Strategy of Aza-Cycles from N-Fused Bicyclo α-Hydroxy-β-lactam, 1

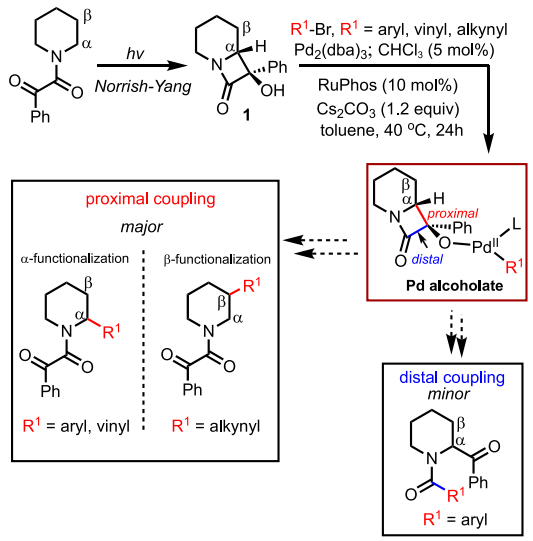

Notably, the α- vs β-functionalization outcome in the studies by Sarpong and co-workers[9] appears to be substrate-controlled. For example, aryl and vinyl bromide coupling partners led to α-functionalization, whereas the β-alkynylation product was obtained using bromoethynyl triisopropylsilane (TIPS-alkynyl-Br) as the coupling partner (see R^1 = alkynyl, proximal coupling product in Scheme 2). In contrast, the selectivity for α- vs β-functionalization observed by Baudoin and co-workers was shown to be controlled by the nature of the ligands: rigid biaryl phosphines led to α-arylated products whereas more flexible biaryl phosphines resulted in β-arylated products (Scheme 1, eq 1).[4a] On the other hand, the palladium-catalyzed γ-selective arylation of piperidines reported by Sanford and co-workers (Scheme 1, eq 4) was mostly controlled by additives.[10] For example, CsOPiv instead of AgOPiv as an additive significantly increased the yield and selectivity for the γ-arylated product.[10]

Ultimately, an in-depth understanding of the roles of ligands, coupling partners, and additives is required in order to predict the outcome of these Pd-catalyzed piperidine functionalization reactions. This knowledge would provide novel design principles for the selective functionalization of piperidines and other aza-cycles. Sarpong and co-workers[9] as well as Baudoin and co-workers[4a] utilized modular Phos ligands (Scheme 3a) possessing highly tunable electronic and steric

Scheme 3. Schematic Presentation of the (a) Buchwald Type of Phos Ligand and Its Possible Binding Modes to the (b) bis-Ligated, and (c) Tris-Ligated Precursor Pd(II)-Complexes

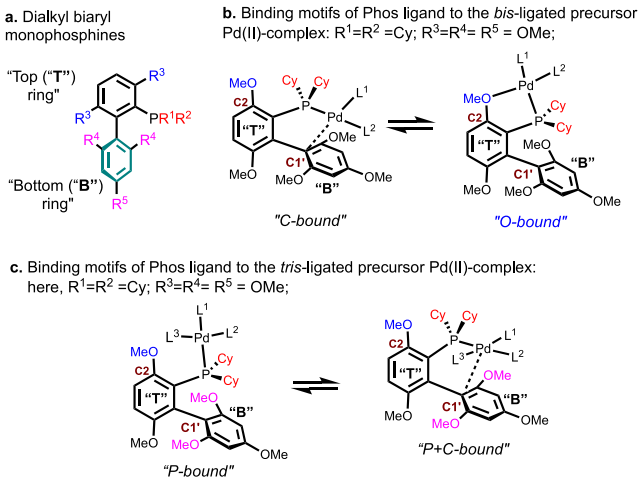

parameters.[13] As has been established, modification of the substituents on the phosphorus and aryl rings of these ligand types significantly impacts their coordination chemistry. In particular, it has been shown[13] that the coordination of Phos ligands to bis-ligated-Pd complexes can lead to two isomeric forms of the resulting tetra-coordinated Pd complex (Scheme 3b).

One binding mode leads to a "C-bound" complex, where two coordination sites are occupied by phosphorus and the bottom phenyl ring (referred to as "B", below) of the ligand. Alternatively, the interaction of Pd with an alkoxy donor atom of the top phenyl group (referred to as "T") of the ligand would lead to an "O-bound" complex. However, little is known about the coordination of the Phos ligands to a tris-ligated-Pd-center. It is expected that the coordination of the ligand to a three-coordinate Pd-center would result in either a tetra-coordinated "P-bound" complex with P atom as the fourth ligand (Scheme 3c) or a penta-coordinated "P,C-bound" complex with P atom and the "B"-ring as the fourth and fifth ligand. The "B"-ring of the ligand can interact with the Pd in several ways or with the lone pairs of the RO-substituents.[14]

In reported catalytic cycles involving biaryl phosphine ligands such as those illustrated in Scheme 3,[13] the coordination environment around the Pd-center can change during the course of the reaction. Therefore, the flexible coordination motif of the Phos ligands is likely to significantly impact not only the reactivity but also the selectivity of the elementary reactions mediated by these complexes. This hypothesis is supported by the findings of Sarpong and co-workers[9] who observed that RuPhos (see Figure 1) favors proximal lactam ring opening of **1** (Scheme 2; proximal C−C bond cleavage proceeds with 10:1 regioselectivity), whereas

https://dx.doi.org/10.1021/jacs.0c10220
J. Am. Chem. Soc. 2020, 142, 21140−21152

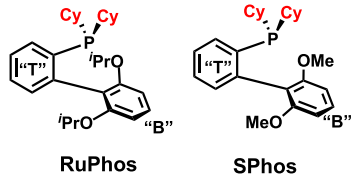

Figure 1. RuPhos and SPhos ligands employed in this study.

SPhos (i.e., OMe instead of ^{i}PrO groups; Figure 1) diminishes yields and regioselectivity to 2:1 (proximal:distal). An in-depth understanding of the electronic and coordination parameters of the Phos ligands will enable the design of ligands that lead to a higher selectivity for proximal vs distal cleavage of substrates such as **1**.

Several key mechanistic features of the reaction developed by Sarpong and co-workers[9] (Scheme 2) still remained to be addressed. The major goals of this Article are to identify factors that control distal vs proximal regioselective C−C cleavage and α- vs β-selectivity in the cross-coupling by understanding the roles of exogenous base additives and the Phos ligands. In the initial report for this transformation,[9] a four-step mechanism for piperidine α-arylation was proposed as illustrated in Scheme 4: (1) oxidative addition of Pd(0) to an aryl halide,

Scheme 4. Previously Proposed Catalytic Cycle

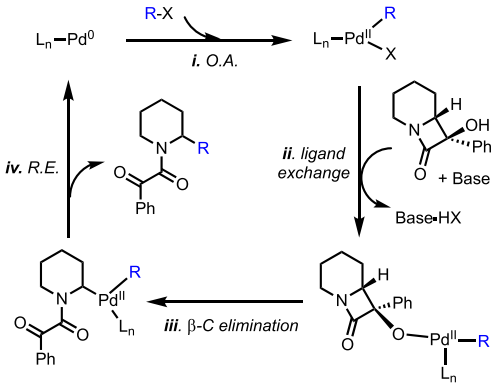

Reproduced from ref 9. Copyright 2020 American Chemical Society.

(2) coordination/deprotonation of the tertiary hydroxy group of **1** to form a Pd-alcoholate, (3) β-carbon elimination to liberate an α-palladated piperidine, and (4) reductive elimination to regenerate the active Pd(0) catalyst and the desired α-arylated product. Here, we investigate each of these elementary steps in detail by computation.

Through our studies, we have now garnered support for (a) the formation of a complex ([(**1**)(Cs_2CO_3)]-PdL(PhBr)) prior to a "*base-mediated oxidative addition*," (b) Cs-carbonate, rather than a halide ligand on Pd, deprotonating the tertiary alcohol in the lowest energy pathway en route to Pd-alcoholate, (c) steric repulsion between the "B"-ring of the Phos ligand and the piperidine ring of **1** as well as donor−acceptor interactions between the "B"-ring and Pd-center (at the regioselectivity-determining β-lactam ring opening transition states) controlling distal vs proximal β-lactam ring opening. On the basis of the latter insight, we predict that reactions using Phos ligands bearing OCF_3 or OCF_2H substituents would be more selective toward proximal ring opening. Finally, we have discovered that the α- vs β-selective cross-coupling on the piperidine ring of **1** depends on the sterics exerted by the coupling partner.

COMPUTATIONAL DETAILS

Geometry and frequency calculations for all reported structures were performed with the Gaussian-16 suite of programs[15] at the [B3LYP-D3(BJ)]/[6-31G(d,p) (for C, H, O, N, and P) +Lanl2dz (Pd, Cs, and Br)] level of theory with the corresponding Hay−Wadt effective core potential[16] for Pd, Cs, and Br (referred to as B3LYP-D3(BJ)/BS1). Thus, here we used the B3LYP[17] density functional with Grimme's empirical dispersion-correction (D3)[18] and Becke−Johnson (BJ)'s damping schemes.[19] Bulk solvent effects were incorporated in all calculations (including the geometry optimization and frequency calculations) at the self-consistent reaction field polarizable continuum model (IEF-PCM)[20] level. We chose toluene as the solvent as it was employed in the laboratory experiments.[9]

The reported energies are at the [B3LYP-D3(BJ)]/BS2 level of theory, where BS2 = [6-311++G(d,p)] (for C, H, O, N, and P)+SDD (for Pd, Cs, and Br), and Stuttgart group effective core potential for Pd, Cs, and Br.[21] The [B3LYP-D3(BJ)]/BS2 calculations are performed at the [B3LYP-D3(BJ)]/BS1 calculated geometries. The presented energies include the [B3LYP-D3(BJ)]/BS1 calculated enthalpy and entropy corrections. While we present the calculated relative energies as $\Delta G/\Delta H$ (in kcal/mol), we discuss only the Gibbs free energies. Calculated Cartesian coordinates of all systems are provided in the Supporting Information. 3D geometries were prepared using CYLView software.[22] NEDA analyses were performed using NBO-7.0. Noncovalent interaction analyses (NCI)[23] were performed using the multiwfn program[24] and VMD software.[25] For

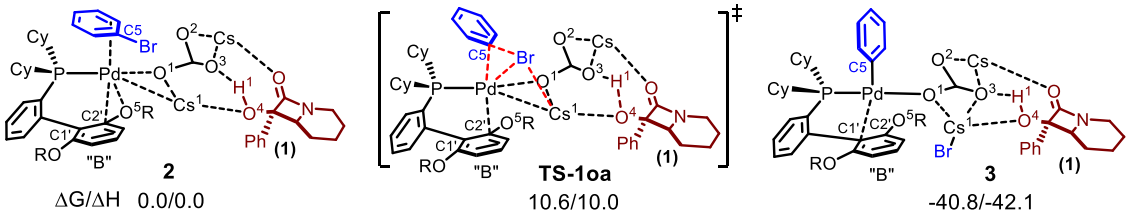

species	Pd-P	Pd-C^5	Pd-Br	C^5-Br	Pd-O^1	Cs^1-Br	Pd-C1'	Pd-C2'	Pd-O^5	O^3-H^1	O^4-H^1
2	2.210	4.410	5.435	1.988	2.155	3.954	3.367	3.150	3.232	1.402	1.068
TS-1oa	2.256	2.483	3.255	2.066	2.276	3.773	3.380	3.403	3.653	1.058	1.445
3	2.274	2.001	4.676	4.904	2.113	3.651	2.671	2.893	3.470	1.413	1.057

Figure 2. Energetically lowest complex (**2**) en route to oxidative addition, Ph−Br oxidative addition transition state (**TS-1oa**), and oxidative addition product **3** with their key geometry parameters (distances are in Å) and relative energies (presented as $\Delta G/\Delta H$ in kcal/mol). Cy = cyclohexane; R = ^{i}Pr. Delocalized (dashed) bonds are omitted from the carbonates for clarity.

https://dx.doi.org/10.1021/jacs.0c10220
J. Am. Chem. Soc. 2020, 142, 21140−21152

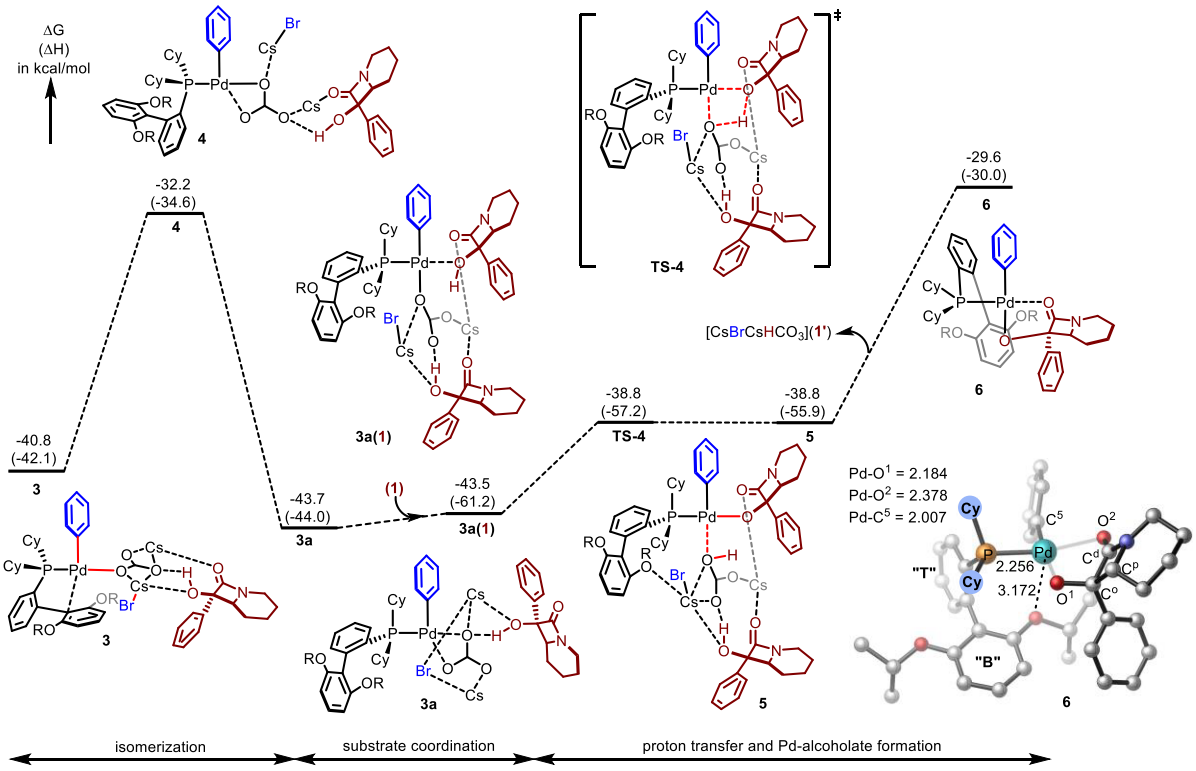

Figure 3. Potential energy surface (PES) of the Pd-alcoholate formation starting from the oxidative addition adduct **3** (energies are given relative to the dissociation limit of **1** + **2**). Bond distances are given in Å. Delocalized (dashed) bonds are omitted for the carbonates for clarity.

the computational studies, we used Cs_2CO_3 as the base rather than its derivatives (e.g., $CsHCO_3$, CsOH, or aggregate forms[26]) that may be present in situ.

RESULTS AND DISCUSSION

Ph−Br Oxidative Addition. Our computations bear out that the initial oxidative addition step of the overall sequence depicted in Scheme 4 involves (a) the formation of a reactive intermediate from a mixture of $Pd_2(dba)_3$ as a precatalyst, RuPhos (L) as a ligand, PhBr as a coupling partner, Cs_2CO_3 as a base, and **1** as a substrate followed by (b) oxidative addition of Ph−Br to the Pd-center. Specifically, our extensive calculations (see the Supporting Information) have established that the low energy complex (**1**)(Cs_2CO_3)-PdL(PhBr) (**2**, Figure 2) forms en route to oxidative addition. The formation of **2** is exergonic by 32.7 kcal/mol relative to the dissociation limit (i.e., PdL + **1** + Cs_2CO_3 + PhBr).[27] Previously,[9] we demonstrated that Cs-cations (from Cs_2CO_3) coordinated to the oxygen of the α-hydroxy β-lactam with simultaneous deprotonation of the α-hydroxy group by CO_3^{2-}. However, in **2**, because of the interaction of the Cs_2CO_3 with the Pd-center, deprotonation of **1** is not completed, albeit the O^4−H^1 bond is elongated to 1.068 Å. Furthermore, in **2**, the Phos ligand is coordinated to the Pd-center through phosphorus (Pd−P = 2.210 Å) and the C2′−OR bond of the "bottom" (i.e., "B") ring (Pd−C2′ = 3.150, and Pd−O = 3.232 Å for R = ^{i}Pr; i.e., RuPhos).

The calculated free energy barrier to traverse **TS-1oa**, relative to complex **2**, is only 10.6 kcal/mol (Figures 2 and S1). Intriguingly, the calculated intrinsic reaction coordinate (IRC) from **TS-1oa** leads to adduct **3**, where the Br atom resides on one of the cesium atoms. Thus, this oxidative addition process is an example of a "*base-mediated oxidative addition*," as previously described by Musaev and co-workers[28] as well as Liu and co-workers.[29] Notably, H^1, which was located within hydrogen bond distance of O^3 in prereaction complex **2**, transfers to the carbonate in **TS-1oa**. In the oxidative addition adduct **3**, O^4 is reprotonated.

Thus, during the reaction **2** → **TS-1oa** → **3**, the proton shuttles between the β-lactam and carbonate, and facilitates the oxidative addition process.[30] The importance of such a H-bonding interaction in catalysis has also been recently reported by Musaev and co-workers,[31] as well as Chang and co-workers.[32] Overall, the reaction **2** → **TS-1oa** → **3** is exergonic by 40.8 kcal/mol.[33]

Notably, our calculations using the model reactions depicted in eqs 5 and 6 (see Figures S2 and S3 for details) and comparison with **2** → **TS-1oa** → **3** show that (a) the addition of Cs_2CO_3 to the reaction mixture (i.e., comparing the free energies of **TS-2(Ph−Br)** and **TS-3(Ph−Br)**) increases both the oxidative addition barrier (from 6.6 to 11.8 kcal/mol) and exergonicity of the reaction (from 32.1 to 44.1 kcal/mol)[34] and (b) the presence of H^1-bonding in **TS-1oa** lowers the free energy barrier by 1.2 kcal/mol for the Ph−Br oxidative addition process.

$$\text{PdL(PhBr)} \rightarrow \textbf{TS-2(Ph-Br)} \rightarrow \text{(Ph)BrPdL} \quad (5)$$

$$(Cs_2CO_3)\text{PdL(PhBr)} \rightarrow \textbf{TS-3(Ph-Br)} \rightarrow \text{(Ph)PdL(BrCsCsCsCO}_3) \quad (6)$$

While the base-mediated oxidative addition is associated with a higher kinetic barrier, it is the likely pathway since, under the conditions employed here, the energetically most

https://dx.doi.org/10.1021/jacs.0c10220
J. Am. Chem. Soc. 2020, 142, 21140−21152

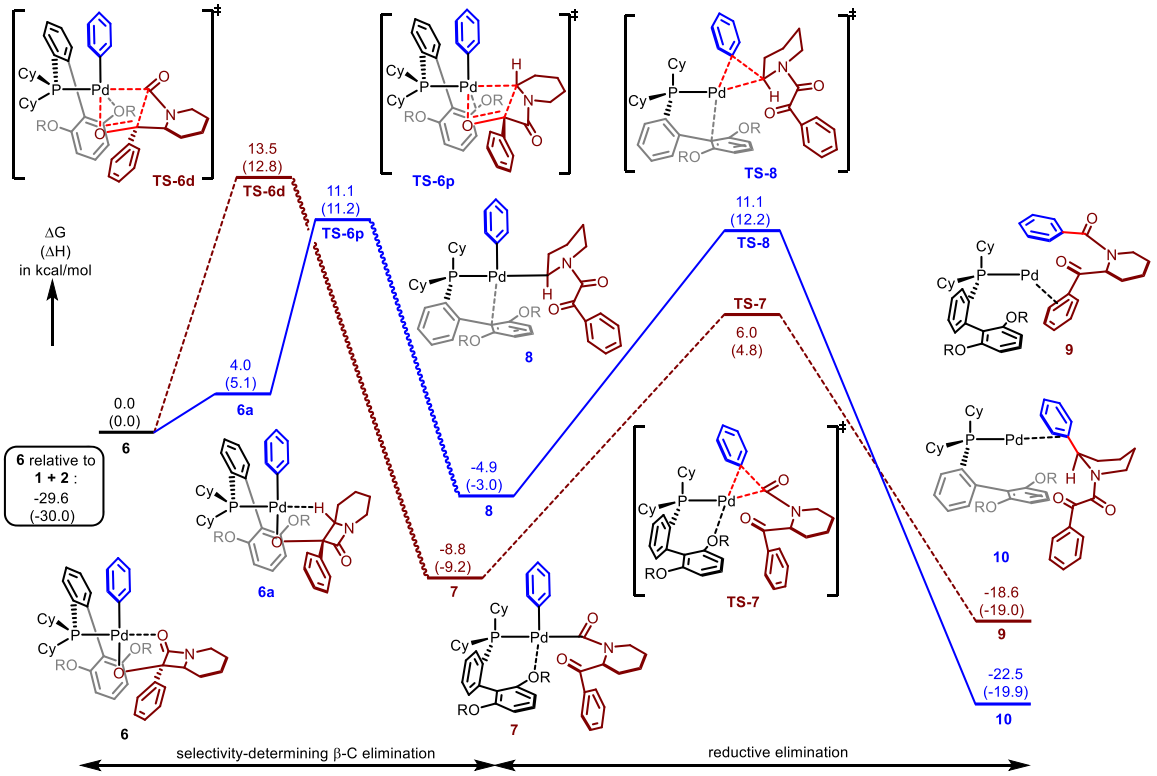

Figure 4. PES for the *β*-carbon elimination and reductive elimination steps.

favorable complex (**1**)(Cs_2CO_3)-PdL(PhBr) (**2**) forms as the reaction initiating complex.

Pd-Alcoholate Formation. Following oxidative addition, adduct **3** engages a second equivalent of substrate, ultimately resulting in the formation of Pd-alcoholate **6** (Figure 3). In **3**, the Pd-center is coordinatively saturated, therefore one (or more) coordinated ligands would need to depart to accommodate an incoming second molecule of the substrate. This ligand reorganization process might proceed via either associative or dissociative pathways. It is well established that the energy required for the dissociative process can be considered as the upper limit of the barrier needed for the associative process, which may require a lower energy barrier.[35] With this in mind, we have investigated several dissociative ligand exchange pathways, among which the dissociation of the "B"-ring of the ligand has the lowest free energy (8.6 kcal/mol) and is most probable (see Figure 3). The resulting intermediate (**3a**) is a more stable oxidative addition product, which then binds another equivalent of substrate followed by displacement to give Pd-alcoholate **6**. As illustrated in Figure 3, all elementary steps of the reaction (**3a** + **1**) → **6** are facile, and the overall process is endergonic by 14.1 kcal/mol. Therefore, we expect the (**3a** + **1**) dissociation limit to be the resting state for the reaction of complex **2** with substrate **1**. On the basis of these findings, below, we calculate the regioselectivity controlling distal (i.e., C^o-C^d) and proximal (i.e., C^o-C^p) bond cleavage barriers[36] either relative to the energetically lowest isomer of Pd-alcoholate (i.e., **6**)[37] or relative to the resting state of the Ph−Br oxidative addition reaction (i.e., **3a** + **1**).

***β*-Carbon Elimination and Reductive Elimination.** Computations show that the distal C^o-C^d bond cleavage occurs at transition state **TS-6d** (Figures 4 and 5) with a free energy barrier of 13.5 kcal/mol, and leads to complex **7**. This

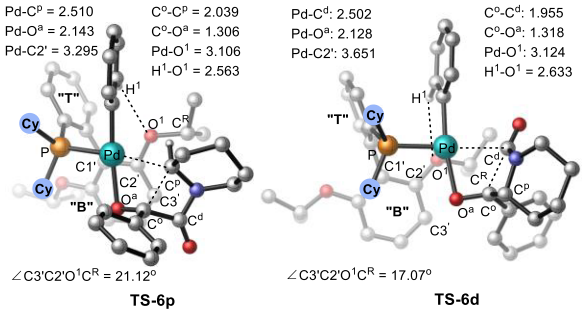

Figure 5. Calculated proximal and distal C−C cleavage transition states **TS-6p** and **TS-6d** for Pd-alcoholate complex **6** (key bond distances are given in Å. Hydrogen atoms and cyclohexane (Cy) rings are omitted for clarity).

elementary reaction is exergonic by 8.8 kcal/mol (see also Figure S5). Alternatively, proximal C^o-C^p bond cleavage occurs via transition state **TS-6p** (Figures 4 and 5) with a lower (by 2.4 kcal/mol) free energy barrier (11.1 kcal/mol) and leads to intermediate **8**. Overall, the kinetically most accessible process is **6** → **8**, which is exergonic by 4.9 kcal/mol. The predicted regioselectivity (proximal cleavage) for **1** reacting with PhBr, on the basis of the energy difference between the regioselectivity controlling transition states (**TS-6d** or **TS-6p**), is in good agreement with the experimentally observed[9] distribution of products (9.8:1 for proximal: distal).

Following *β*-carbon elimination, the next step is the C−C reductive elimination. For the distal pathway (shown in brown, Figure 4), C−C reductive elimination proceeds via transition state **TS-7** with a 14.8 kcal/mol free energy barrier and is exergonic by 9.8 kcal/mol, relative to intermediate **7**. For the proximal pathway (shown in blue, Figure 4), the C−C reductive elimination from **8** has an associated 16.0 kcal/mol

https://dx.doi.org/10.1021/jacs.0c10220
J. Am. Chem. Soc. 2020, 142, 21140−21152

free energy barrier (at the transition state **TS-8**) and is exergonic by 17.6 kcal/mol, relative to intermediate **8**.

Next, we elucidate the influence of the Phos ligands on the relative energy of the regioselective ring opening transition states.

Factors Impacting Proximal vs Distal β-Carbon Elimination. There are several factors that impact the calculated energies of the proximal vs distal regioselectivity controlling transition states **TS-6p** and **TS-6d** (see Figure 5). As previously identified by us,[9] among these factors are (a) the difference in the proximal and distal C−C bond strengths, (b) the nature of the aryl substituent on the α-hydroxy-β-lactam, **1**, and (c) the nature of the Phos ligand. An understanding of these factors is critical to establishing a full appreciation of distal vs proximal regioselective cleavage in the β-carbon elimination step. Previously, we have described some of these factors (see also Figure S6).[9] However, the impact of the nature of Phos ligand on proximal vs distal ring-opening, as well as the factors controlling the α vs β site-selective cross-coupling of the piperidine moiety in **1** had not been studied and are described here.

Close examination of transition states **TS-6d** and **TS-6p** revealed differences in (a) the positioning of the piperidine and the "B"-ring of the ligand as well as (b) the nature and strength of the Pd−"B"-ring interaction, which was influenced by the steric repulsion between the piperidine moiety of the substrate and "B"-ring of the ligand ("steric-induced electronic" and "stereoelectronic" interactions).[38] To better understand the steric, electronic, and stereoelectronic effects, we first performed distortion-interaction analyses of **TS-6d** and **TS-6p**.[39] For this purpose, we partitioned each transition state into two parts: substrate (*sub*, blue, in Figure 6), including the (Ph)Pd(Piperidine) fragment, and *ligand* (black, in Figure 6); here we used RuPhos as a ligand (see also Figure S7).

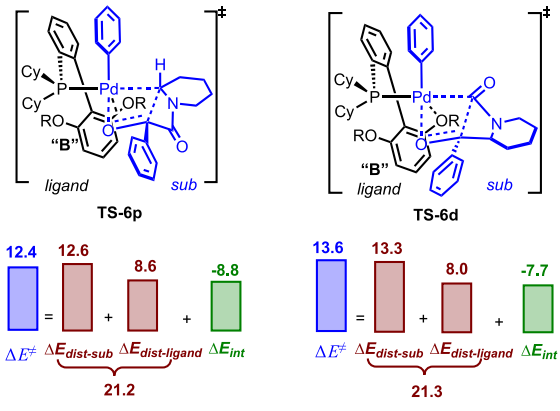

Figure 6. Distortion/interaction analysis of the regioselectivity controlling C−C cleavage transition states **TS-6p** and **TS-6d** (energies are in kcal/mol, and $\Delta E^{\ddagger}$ is relative to **6**).

Calculations show that the distortion of the *ligand* ($\Delta E_{\text{dist-}ligand}$) in **TS-6p** (8.6 kcal/mol) is slightly larger than that in **TS-6d** (8.0 kcal/mol). This is manifested in the calculated (C3′,C2′,O^1,C^R) dihedral angle, which is 21.12° and 17.07° in **TS-6p** and **TS-6d**, respectively (Figure 5). Thus, the OR substituent of the "B"-ring of the ligand is rotated further down in **TS-6p** than in **TS-6d**, because of the relatively strong steric repulsion between the substrate and "B"-ring of the ligand. This is evident in the examination of the calculated structure shown in Figure 5. Of course, this rotation impacts the positioning of the lone-pair π-orbitals of the ligand O-atoms, (as well as the aromatic π-orbitals of the "B"-ring; see Schemes 3 and 5), which would be manifested in the

Scheme 5. Representative Orbitals Participating in the Pd−O and Pd−(C2′-O) Donor−Acceptor Interactions[a]

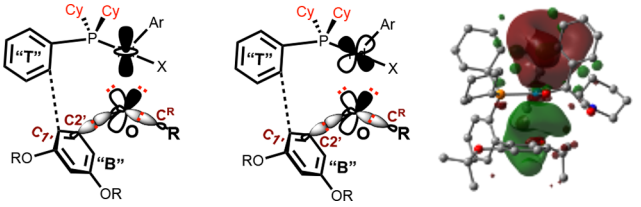

[a]The orbitals of the oxygen lone pairs (LPs), C−O bonds (for C2′ and CR), and the π bonds of the "B"-ring are shown in Figure S8.

calculated Pd−O and Pd−C2′ bond distances in these transition states: in **TS-6p**, the Pd−O^1 and Pd−C2′ distances are 3.106 and 3.295 Å, but in **TS-6d** they are 3.124 and 3.651 Å, respectively (Figure 5). Although the calculated total distortion ($\Delta E_{\text{dist-}sub} + \Delta E_{\text{dist-}ligand}$) energies for **TS-6p** and **TS-6d** are nearly the same (21.2 and 21.3 kcal/mol, respectively), the observed change in the Pd−O and Pd−C2′ bonding as well as the nature of the ligand distortion (i.e., rotation down of the R-group of the OR-substituent) are expected to be major contributors to the calculated *sub*−*ligand* interaction energies. Consistent with this hypothesis, the calculated electronic interaction energy (ΔE_{int}) between the *ligand* and *sub* fragments is 1.1 kcal/mol more favorable in **TS-6p** than in **TS-6d** (see Figure 6). In addition, there is also a weak H-bonding interaction (H^1−O^1 distance of 2.563 and 2.633 Å, in **TS-6p** and **TS-6d**, respectively, Figure 5) between the Pd-coordinated Ph and O-center of the OR-substituent. To provide additional support for the analysis presented above and identify other factors that possibly impact the interaction between the *sub* and *ligand* fragments in **TS-6p** and **TS-6d**, we also performed natural energy decomposition analysis (NEDA) calculations.[40] These studies (see the Supporting Information for more details) have identified that

(a) weak interactions (e.g., van der Waals, dipole−dipole, and dipole−(induced dipole)), combined under the electrical interaction (EL) term, do not contribute significantly to the calculated energy difference between **TS-6p** and **TS-6d**, and

(b) a charge transfer (CT) interaction between the *ligand* and *sub* fragments contributes significantly to the calculated total electronic energies of **TS-6p** and **TS-6d**: it is 8.1 kcal/mol larger in **TS-6p** than in **TS-6d**.

To provide more support for the above proposed "stereoelectronic" interaction concept, we have calculated the second order perturbative interaction energies, $E^{(2)}_{ij}$, between the (a) Pd-center and oxygen of the OR-group, (b) Pd-center and C2′−OR bond (combined with the C^R−OR bond), and (c) Pd-center and "B"-ring of the ligand. We found that these interaction energies are 4.8, 5.4, and 7.4 kcal/mol in **TS-6p**, and 6.2, 2.6, and 2.4 kcal/mol in **TS-6d**, respectively. Altogether, the total donor−acceptor interactions are 17.6 and 11.2 kcal/mol, respectively,[41] for **TS-6p** and **TS-6d**, which is consistent with the geometry changes in **TS-6p** and **TS-6d** presented above (see also the Supporting Information).

https://dx.doi.org/10.1021/jacs.0c10220
J. Am. Chem. Soc. 2020, 142, 21140−21152

Table 1. Calculated Free Energy Difference ($\Delta\Delta G^{\ddagger}$, in kcal/mol) between Regioselectivity Controlling Transition States TS-6p and TS-6d, as Well as Key Geometry Parameters (Dihedral Angle in Degrees and Bond Distance in Å), with Phos Ligands Bearing R = Me, CF_3, CF_2H, ^{t}Bu, and Ad Substituents

		∠(C3′, C2′, O^1, C^R)		Pd−O^1		Pd−C2′	
R	$\Delta\Delta G^{\ddagger}$	TS-6p(R)	TS-6d(R)	TS-6p(R)	TS-6d(R)	TS-6p(R)	TS-6d(R)
Me	1.6	−6.26	0.98	4.410	2.977	3.697	3.533
^{i}Pr	2.4	21.12	17.07	3.106	3.124	3.295	3.651
CF_3	4.0	73.73	17.05	2.860	2.995	3.473	3.420
CF_2H	3.4	69.42	21.25	2.855	2.964	3.465	3.434
^{t}Bu	0.6	74.49	58.55	2.911	2.842	3.403	3.405
Ad	−0.7	102.17	126.91	3.039	2.879	3.510	3.517

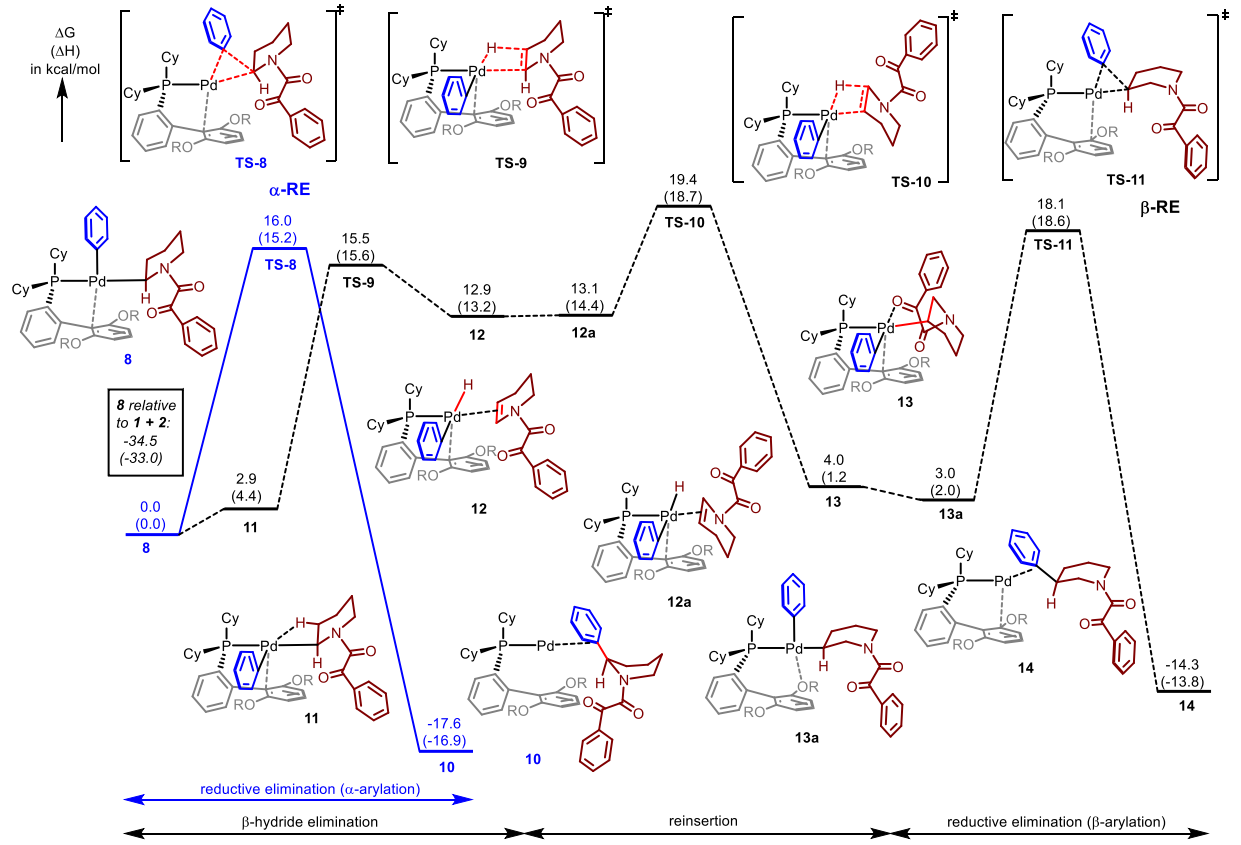

Figure 7. PES of the α- (blue) vs β-arylation (black) pathways.

Prediction of New Phos Ligands for Selective Proximal vs Distal Ring Opening in 1. To validate our proposed "*steric enabled electronic effects from the Phos ligand; SEEEL*" that explains the selective proximal vs distal ring opening in **1**, we have examined other Phos ligands bearing different OR-substituents with R = Me, CF_3, CF_2H, ^{t}Bu, and Ad. For these systems, we calculated the selectivity controlling transition states and associated prereaction complexes (see Table 1).[42]

Consistent with the SEEEL concept, the proximal vs distal ring opening in **1** should be less selective when the R-substituent of the Phos ligands is smaller than ^{i}Pr: indeed, the calculated free energy difference, $\Delta\Delta G^{\ddagger}$, between the selectivity controlling transition states is smaller for R = Me (i.e., SPhos) than for the R = ^{i}Pr (i.e., RuPhos). On the basis of this analysis, the Pd/SPhos-mediated proximal vs distal ring opening in **1** is anticipated to be less selective than with RuPhos as ligand. This conclusion is consistent with our previously reported experimental data which show that reactions employing RuPhos are more selective (9.8:1) than SPhos (2:1) toward proximal ring opening.[9]

The calculated geometry parameters of **TS-6d(Me)** and **TS-6p(Me)** (i.e., with SPhos ligand) are generally consistent with the predictions above. Indeed, in both **TS-6d(Me)** and **TS-6p(Me)**, there are smaller steric repulsions between the "B"-ring (i.e., with its OMe substituent) and piperidine moiety (see Table 1 and Figures S9 and S10), which is manifested in the much smaller (C3′,C2′,O^1,C^R) dihedral angles (compared to the case with R = ^{i}Pr). Interestingly, in the proximal C−C cleavage transition state **TS-6p(Me)**, this dihedral angle has a negative value of −6.26°. In this case, the Me group has rotated in the "opposite" direction, i.e., an "up mode," because of the presence of strong H-bonding between the Pd-coordinated Ph and O^1-center of the O^1R-substituent (H^1−O^1 = 2.173 Å; see Figures S9 and S10).

https://dx.doi.org/10.1021/jacs.0c10220
J. Am. Chem. Soc. 2020, 142, 21140−21152

We have also applied the SEEEL regioselectivity concept to Phos ligands with R = CF_3, CF_2H, ^{t}Bu, and Ad substituents. Data presented in Table 1 show that the use of the ligands with the trifluoromethoxy (OCF_3) and oxidifluoromethyl (OCF_2H) substituents would significantly improve selectivity for proximal over distal ring opening in **1**: the calculated free energy differences, $\Delta\Delta G^{\ddagger}$, between the selectivity controlling transition states are 4.0 and 3.4 kcal/mol for R = CF_3 and OCF_2H, respectively.[43] Furthermore, the calculated key geometry parameters of the associated transition states (see Table 1 and Figure S10) are fully consistent with the SEEEL concept presented above. Additional effects may also account for the computed higher selectivity for ligands with the R = CF_3 or OCF_2H. For example, the greater acceptor ability of the σ^*(C−O) orbital in these cases could lead to a significant Pd → σ^*(C−O) back bonding.[44] On the basis of the calculated Pd−O bond distances (see Table 1), such an interaction is more pronounced in the proximal C−C cleavage transition state than in the distal case, leading to a higher level of interaction.

Next, we sought to elucidate the impact of bulkier R-groups (*tert*-butyl, ^{t}Bu, and adamantyl, Ad) of the Phos ligand on the selectivity of proximal vs distal ring opening in **1**. The presence of the larger R-substitutions results in significant steric repulsion between the "B"-ring of ligand (and its OR-group) and piperidine moiety of substrate, in both proximal and distal C−C cleavage transition states, leading to large calculated dihedral angles (C3′,C2′,O^1,C^R). Such a large rotation of the OR groups (see Table 1) makes fully available the donor orbitals of the O^1-center that results in equally strong Pd−O^1 interactions in both proximal and distal transition state structures. Consistent with these geometry deformations, the calculated free energy difference, $\Delta\Delta G^{\ddagger}$, of the transition states leading to the proximal and distal ring opening products becomes very small. Therefore, it is predicted that selectivity for proximal vs distal ring opening in **1** using Phos ligands bearing O^{t}Bu and OAd substituents will be minimal.

Site Selectivity: α- vs β-Functionalization. We have also sought insight into the factors controlling the site-selective cross-coupling step, i.e., the α-, β-, or γ-selective functionalization, of the piperidine moiety in **1** and related substrates. Previously, we demonstrated that α- or β-selectivity in the coupling step had a dependence on the cross-coupling partners; aryl and vinyl bromide coupling partners led to α-functionalization, whereas bromoethynyl triisopropylsilane (TIPS-alkyne-Br) led to β-alkynylation (Scheme 2). In contrast, the α- vs β-functionalization of related piperidine systems reported by Baudoin and co-workers was controlled by the ligand. In those cases, rigid biaryl phosphines led to α-arylated products whereas more flexible biaryl phosphines resulted in β-arylated products (Scheme 1, eq 1).[4a] Below, we provide some insights into the factors that control selectivity for the couplings reported by us.[9] Our analysis started with the previously proposed mechanism for Pd-catalyzed β-arylation proposed by Knochel and co-workers[3] and Baudoin and co-workers,[4a] which begins from an α-palladated intermediate that undergoes β-hydride elimination, reinsertion, and reductive elimination.

The α- and β-Selective Arylation of the Piperidine in 1. As shown in Figures 4 and 7, the α-arylation of the piperidine in **1** starts from intermediate **8** and proceeds via reductive elimination transition state **TS-8** (also referred to as α-RE) to produce **10**. The overall free energy barrier of this process is 16.0 kcal/mol, and the α-arylation reaction (**8** → **TS-8** → **10**) is exergonic by 17.6 kcal/mol (Figure 7, blue).

For β-arylation to occur, intermediate **8** should, at first, convert to intermediate **11**. This requires the Pd-bound phenyl group (shown in blue in structure **8**) to rearrange from the axial to the equatorial position with concomitant formation of a β-C−H agostic interaction (with Pd···H and C−H bond distances of 2.405 and 1.108 Å, respectively; see Figure S11). The rearrangement of **8** → **11** is endergonic by 2.9 kcal/mol, and the β-hydride elimination that follows (i.e., formation of π-complex **12**) via transition state **TS-9** is 15.5 kcal/mol higher than intermediate **8**. As previously shown,[4,45] in order for the alkene group to reinsert into the Pd−H bond, a rearrangement of intermediate **12** to **12a** is required: this is calculated to occur with almost no energy barrier. The ensuing reinsertion of the alkene into the Pd−H bond via **TS-10** leads to four-coordinate intermediate **13**, where the ketoamide ketone group is coordinated to the Pd-center (Pd−O = 2.339 Å, see Figure S11). Intermediate **13** isomerizes to **13a** with almost no energy barrier: in **13a** the phenyl group and the C−H bond at the carbon bearing Pd are trans to each other. At this stage, C−C reductive elimination occurs via **TS-11** (also referred to as β-RE) and leads to β-arylated product **14**. The free energy surface associated with the β-arylation reaction, i.e., **8** → **14**, has an overall 19.4 kcal/mol free energy barrier (at the double bond reinsertion transition state **TS-10**) and is exergonic by 14.3 kcal/mol. Thus, these calculations support the Pd/RuPhos-catalyzed coupling of **1** with PhBr as α-selective: the β-arylation would have a 3.4 kcal/mol higher free energy barrier at the reinsertion transition state **TS-10**.

The vinylation of piperidine **1** was calculated to occur through similar intermediates and transition states, predicting a preference for the α-vinylation product by 3.3 kcal/mol (see Tables 2 and S2). This finding is also consistent with our empirical observations.[9]

Table 2. Calculated Free Energy Barriers (in kcal/mol) for the Key Steps of the Piperidine α- and β-Selective Arylation, Vinylation, and Alkynylation with Aryl-Br, Vinyl-Br, TIPS-Alkynyl-Br, C(^{i}Pr)$_3$-Alkynyl-Br, and Ethynyl-Br Substrates

substrates	α-RE	β-hydride elimination	reinsertion	β-RE
aryl	16.0	15.5	19.4	18.1
vinyl	13.1	13.9	16.4	13.3
TIPS-alkynyl	18.0	13.9	12.9	14.9
C(^{i}Pr)$_3$-alkynyl	15.5	5.3	7.1	12.9
ethynyl	14.7	10.1	13.9	15.9

The α- and β-Selective Alkynylation of Piperidine in 1. We next calculated the mechanism of the selective β-alkynylation of the piperidine in **1** using TIPS-alkyne-Br as the coupling partner. We found that the alkynylation reaction proceeded through a pathway with intermediates and transition states that were analogous to the arylation case (see Figure S12). The C−C reductive elimination that results in α-alkynylation has an 18.0 kcal/mol free energy barrier (via **TS-ak1**, see Scheme 6) and is exergonic by 13.6 kcal/mol. For β-alkynylation, both the reinsertion (via **TS-ak3**) and C−C reductive elimination at the β-carbon (via **TS-ak4**) are more favorable than the α-alkynylation ($\Delta\Delta G^{\ddagger}$ = 3.1 kcal/mol; see Table 2). This conclusion is consistent with our empirical findings.[9]

Origins of the Substrate-Controlled α- vs β-Selectivity. To establish the origins of the substrate-controlled α- vs β-

https://dx.doi.org/10.1021/jacs.0c10220
J. Am. Chem. Soc. 2020, 142, 21140−21152

Scheme 6. α-RE and β-RE Transition States for Arylation and Alkynylation

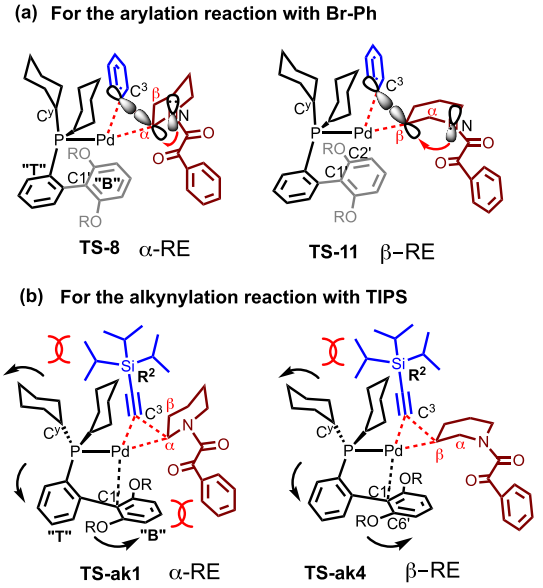

selective C−C cleavage/cross-coupling in **1**, we first analyzed the C−C reductive elimination transition states, α-RE and β-RE.[46] Several factors impact the energies of these transition states. The first of these is the electron-poor nature of the α-carbon relative to the β-carbon of the piperidine moiety, because of its proximity to the N-center in the piperidine ring (see Table 3). This pronounced inductive electron-withdrawing effect favors the β-RE transition state over the α-RE and is independent of the coupling partner.[47] A second, stereoelectronic, effect is the distance-dependent donor−acceptor interaction between the lone-pair of the N-center of piperidine and developing σ^*-orbital of the $C^3-C^{\alpha(\text{or }\beta)}$ bond (see **TS-8** and **TS-11** in Scheme 6 and Table 3). The second-order perturbative interaction analysis clearly shows that the donor−acceptor interaction energy (i.e., $E^{(2)}_{ij}$) between the lone pair of N and adjacent $C^3-C^{\alpha(\text{or }\beta)}$ antibonding σ^*-orbital is larger for α-RE than β-RE. This distance-dependent donor−acceptor effect overrides the inductive effect and favors α-selective reductive elimination.

Again, on the basis of the data presented in Table 3, the second-order perturbative donor−acceptor interaction is only weakly dependent on the nature of the coupling partner. *In summary, the combination of electronic and stereoelectronic effects strongly favor α- over β-selectivity, independent of the nature of the coupling partner.* However, they do not explain the observed β-alkynylation when the TIPS-alkyne-Br coupling partner is used. Here, we believe the preference is sterically driven (see **TS-ak1** and **TS-ak4**, Scheme 6b and Table 3). We have identified two steric factors, which are internally connected. The first is steric repulsion between the Cy rings of the Phos ligand and the coupling group (referred to as a Cy−R^2 interaction).

To minimize the steric clash, the Cy rings rotate out to accommodate the large R^2-substituent (TIPS in the illustrated cases for **TS-ak1** and **TS-ak4**). In general, one would expect that a larger R^2 substituent would lead to a larger Cy−R^2 steric repulsion. The second steric effect involves interaction between the "B"-ring of the ligand and phenyl group of the phenone amide substituent (see **TS-ak1**; referred as a "B"−Ph interaction). This effect is calculated to be larger for α-RE than β-RE. The calculated $C^y-P-Pd-C^3$ dihedral angles (see Table 3) are consistent with these expectations. However, the large Cy−R^2 steric repulsion triggers a stabilizing interaction between the Pd-center and the "B"-ring: this interaction is going to be more pronounced in β-RE than α-RE because of the smaller "B"−Ph steric repulsion in the former.

This is borne out in the calculated Pd−C1′ distance of 2.919 Å for **TS-ak1** (i.e., α-RE) versus 2.708 Å for **TS-ak4** (i.e., β-RE). The pronounced Pd−"B"-ring interaction makes the "B"-ring an emerging fourth coordinated ligand that increases the steric hindrance around the Pd-center and promotes the reductive elimination.

Therefore, the size of the R^2-group is critical for α- versus β-selective alkynylation. Consistent with this hypothesis are the calculated energies of the α-RE and β-RE transition states for the piperidine alkynylation with bromoethyne (i.e., R^2 = H) and bromoethynyl triisopropylmethane (i.e., R^2 = $C(^iPr)_3$). For R^2 = H, which lacks the steric effects, α-selective alkynylation is anticipated by 1.2 kcal/mol. However, for R^2 = $C(^iPr)_3$), which would lead to relatively less pronounced steric effects as compared to R^2 = TIPS, the reaction is still β-selective, but only by 2.6 kcal/mol (3.1 kcal/mol for R^2 = $Si(^iPr)_3$).

Notably, for PhBr, because the aryl ring is positioned perpendicular to the Cy rings of the RuPhos ligand in the α-RE and β-RE transition states, there is less pronounced Cy−Ph steric hindrance (see Table 3). Consequently, the "B"-ring of the ligand is positioned away from the Pd-center in the transition states. As a result, the associated **TS-8** (i.e., α-RE) and **TS-11** (i.e., β-RE) transition states are less sensitive to steric effects in this case. In summary, the α- and β-selective functionalization of the piperidine in **1** is sensitive to the Phos ligand as well as the size of the coupling partner.

CONCLUSIONS

In this Article, we have presented key mechanistic details as well as reactivity and selectivity (regio-, and α- vs β-

Table 3. Calculated Parameters of the α- and β-Selective Reductive Elimination Transition States, α-RE and β-RE[a]

	α-RE						β-RE					
	C^α	C^β	$\Delta G^\ddagger$	$E^{(2)}_{ij}$	DA	Pd−C1′	C^α	C^β	$\Delta G^\ddagger$	$E^{(2)}_{ij}$	DA	Pd−C1′
Ph	−0.16	−0.46	16.0	19.5	22.5	3.139	−0.27	−0.37	18.2	0.9	36.4	3.061
Vin	−0.18	−0.47	13.1	17.0	31.2	3.108	−0.27	−0.38	13.3	2.0	30.6	2.999
$Si(^iPr)_3$	−0.15	−0.47	18.0	21.2	42.3	2.919	−0.26	−0.38	14.9	2.1	45.0	2.708
H	−0.15	−0.46	14.7	21.4	15.6	2.941	−0.26	−0.36	15.9	2.3	24.7	2.936
$C(^iPr)_3$	−0.14	−0.47	15.5	20.7	34.5	3.003	−0.26	−0.37	12.9	1.9	47.3	2.971

[a]NBO Charges of α- and β-Carbons Are Given in lel, Energies Are Given in kcal/mol, DA = (C^y,P,Pd,C^3) Dihedral Angle is in Deg., and Pd−C1′ Bond Distance is in Å.

https://dx.doi.org/10.1021/jacs.0c10220
J. Am. Chem. Soc. 2020, 142, 21140−21152

Scheme 7. Proposed Mechanism for the Pd/RuPhos-Mediated C−C Cleavage/Cross-Coupling of N-Fused Bicyclo α-Hydroxy-β-Lactam 1

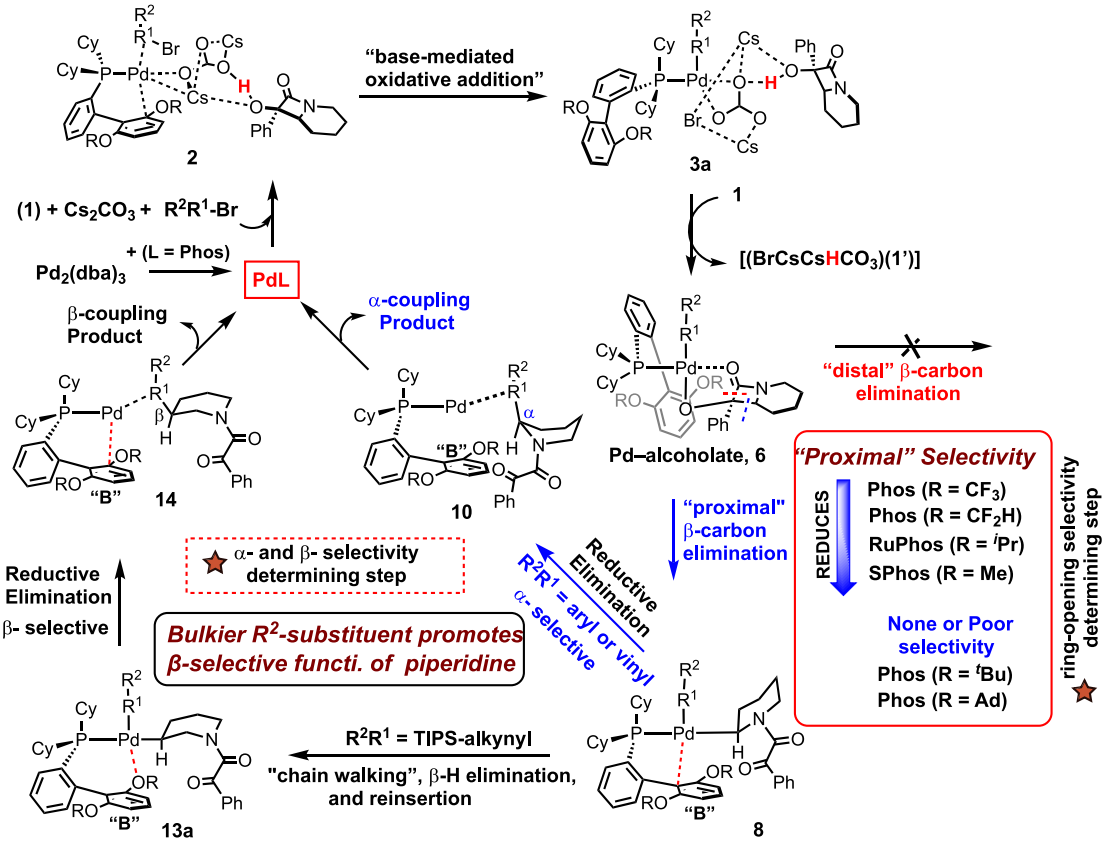

functionalization) controlling factors in the dialkylbiarylphosphine (Phos)/Pd-catalyzed C−C cleavage/cross-coupling of *N*-fused bicyclo α-hydroxy-β-lactam, **1** (see Scheme 7). As illustrated in Scheme 7, we have found the following:

(1) With $Pd_2(dba)_3$ as a precatalyst, RuPhos as a ligand (L), R^2R^1-Br as a coupling partner, Cs_2CO_3 as a base, and **1** as a substrate, an energetically most stable reactive complex [(**1**)(Cs_2CO_3)]-PdL(R^2R^1-Br), **2**, forms prior to the Ph−Br oxidative addition via a *"base-mediated oxidative addition"* mechanism. This reaction occurs with a small free energy barrier and is highly exergonic. The oxidative addition product [($BrCsCsCO_3$)(**1**)]-PdL(R^2R^1), **3a**, with a CsBr fragment, is the resting state en route to Pd-alcoholate (**6**) formation.

(2) β-Lactam ring opening (i.e., the β-carbon elimination) in Pd-alcoholate **6** proceeds preferentially through proximal C−C cleavage. This finding (by utilizing RuPhos as the ligand) is in good agreement with the experimentally observed product distribution (9.8:1 in favor of proximal cleavage).[9]

(3) The newly developed *"steric enabled electronic effects from the Phos ligand; SEEEL"* concept explains the selective proximal vs distal ring opening (i.e., regioselectivity) in **1**. This concept is based on the fact that steric repulsion between the bottom "B"-ring of the Phos ligand and piperidine of the substrate at the regioselectivity-determining β-carbon elimination transition states induces rotation of the R-group, which, in turning, promotes a donor−acceptor interaction between the Pd-center and "B"-ring. This weak stereoelectronic interaction drives the proximal C−C cleavage transition state over the distal one.

(4) The distal vs proximal C−C cleavage in **1** is dependent on the size and electronics of the R-group of the OR substituent of Phos ligand, which is consistent with the SEEEL concept. By utilizing of this concept, we predict that the reactions using Phos ligands bearing OCF_3 and OCF_2H substituents are going to be more selective toward proximal ring opening in **1**.

(5) The α- or β-selective cross-coupling on the piperidine of **1** is sensitive to the size of the R^2-substituent of the coupling partner (for example, TIPS group in TIPS-alkyne-Br). We have shown that the steric clash between the R^2-substituent of the coupling partner and Phos ligand triggers a stabilizing interaction between the Pd-center and "B"-ring, that makes the "B"-ring an emerging fourth coordinated ligand, which, in turn, increases the steric hindrance around the Pd-center and promotes the reductive elimination. The Pd−"B" interaction is more pronounced in β-RE than in α-RE. Thus, the size of R^2-substituent of the coupling partner can be varied to control α- or β-selective cross-coupling in these reactions.

■ ASSOCIATED CONTENT

Supporting Information

The Supporting Information is available free of charge at https://pubs.acs.org/doi/10.1021/jacs.0c10220.

Computational details, energies and frequency analysis, and Cartesian coordinates of all reported structures (PDF)

■ AUTHOR INFORMATION

Corresponding Authors

Djamaladdin G. Musaev − *Cherry L. Emerson Center for Scientific Computation, and Department of Chemistry, Emory University, Atlanta, Georgia 30322, United States;*

https://dx.doi.org/10.1021/jacs.0c10220
J. Am. Chem. Soc. 2020, 142, 21140−21152

orcid.org/0000-0003-1160-6131; Email: dmusaev@emory.edu

Richmond Sarpong − *Department of Chemistry, University of California, Berkeley, California 94720, United States;* orcid.org/0000-0002-0028-6323; Email: rsarpong@berkeley.edu

Authors

Li-Ping Xu − *Cherry L. Emerson Center for Scientific Computation, and Department of Chemistry, Emory University, Atlanta, Georgia 30322, United States; School of Chemistry and Chemical Engineering, Shandong University of Technology, Zibo 255000, China*

Jose B. Roque − *Department of Chemistry, University of California, Berkeley, California 94720, United States;* orcid.org/0000-0002-5449-1584

Complete contact information is available at: https://pubs.acs.org/10.1021/jacs.0c10220

Notes

The authors declare no competing financial interest.

■ ACKNOWLEDGMENTS

This work was supported by the National Science Foundation under the CCI Center for Selective C−H Functionalization (CHE-1700982). The authors gratefully acknowledge the use of the resources of the Cherry Emerson Center for Scientific Computation at Emory University. L.-P.X. acknowledges the Natural Science Foundation of China (NSFC 21702126) and the China Scholarship Council for support. J.B.R. is grateful to Bristol Myers Squibb (BMS) for a graduate fellowship.

■ REFERENCES

(1) (a) Chen, X.; Engle, K. M.; Wang, D.-H.; Yu, J.-Q. Palladium(II)-catalyzed C-H activation/C-C cross-coupling reactions: Versatility and practicality. *Angew. Chem., Int. Ed.* **2009**, *48*, 5094−5115. (b) Lyons, T. W.; Sanford, M. S. Palladium-catalyzed ligand-directed C−H functionalization reactions. *Chem. Rev.* **2010**, *110*, 1147−1169. (c) Giri, R.; Shi, B.-F.; Engle, K. M.; Maugel, N.; Yu, J.-Q. Transition metal-catalyzed C−H activation reactions: diastereoselectivity and enantioselectivity. *Chem. Soc. Rev.* **2009**, *38*, 3242−3272. (d) Wencel-Delord, J.; Dröge, T.; Liu, F.; Glorius, F. Towards mild metal-catalyzed C−H bond activation. *Chem. Soc. Rev.* **2011**, *40*, 4740−4761. (e) Gandeepan, P.; Muller, T.; Zell, D.; Cera, G.; Warratz, S.; Ackermann, L. 3d Transition metals for C-H activation. *Chem. Rev.* **2019**, *119*, 2192−2452.

(2) Coldham, I.; Leonori, D. Synthesis of 2-arylpiperidines by palladium couplings of aryl bromides with organozinc species derived from deprotonation of N-Boc-piperidine. *Org. Lett.* **2008**, *10*, 3923−3925.

(3) Seel, S.; Thaler, T.; Takatsu, K.; Zhang, C.; Zipse, H.; Straub, B. F.; Mayer, P.; Knochel, P. Highly diastereoselective arylations of substituted piperidines. *J. Am. Chem. Soc.* **2011**, *133*, 4774−4777.

(4) (a) Millet, A.; Larini, P.; Clot, E.; Baudoin, O. Ligand-controlled β-selective C(sp^3)−H arylation of N-Boc-piperidines. *Chem. Sci.* **2013**, *4*, 2241−2247. (b) Millet, A.; Dailler, D.; Larini, P.; Baudoin, O. Ligand-controlled alpha- and beta-arylation of acyclic N-Boc amines. *Angew. Chem., Int. Ed.* **2014**, *53*, 2678−2682.

(5) (a) Chen, W.; Ma, L.; Paul, A.; Seidel, D. Direct α-C−H bond functionalization of unprotected cyclic amines. *Nat. Chem.* **2018**, *10*, 165−169. (b) Paul, A.; Seidel, D. α-Functionalization of cyclic secondary amines: Lewis acid promoted addition of organometallics to transient imines. *J. Am. Chem. Soc.* **2019**, *141*, 8778−8782.

(6) Pastine, S. J.; Gribkov, D. V.; Sames, D. sp^3 C−H bond arylation directed by amidine protecting group: α-arylation of pyrrolidines and piperidines. *J. Am. Chem. Soc.* **2006**, *128*, 14220−14221.

(7) Prokopcová, H.; Bergman, S. D.; Aelvoet, K.; Smout, V.; Herrebout, W.; Van der Veken, B.; Meerpoel, L.; Maes, B. U. W. C-2 arylation of piperidines through directed transition-metal-catalyzed sp^3 C-H activation. *Chem. - Eur. J.* **2010**, *16*, 13063−13067.

(8) (a) Jain, P.; Verma, P.; Xia, G.; Yu, J.-Q. Enantioselective amine α-functionalization via palladium-catalysed C−H arylation of thioamides. *Nat. Chem.* **2017**, *9*, 140−144. (b) Jiang, H.-J.; Zhong, X.-M.; Yu, J.; Zhang, Y.; Zhang, X.; Wu, Y.- D.; Gong, L.-Z. Assembling a Hybrid Pd Catalyst from a Chiral Anionic CoIII Complex and Ligand for Asymmetric C(sp^3)−H Functionalization. *Angew. Chem., Int. Ed.* **2019**, *58*, 1803−1807. (c) Greßies, S.; Klauck, F. J. R.; Kim, J. H.; Daniliuc, C. G.; Glorius, F. Ligand-Enabled Enantioselective C−H Activation of Tetrahydroquinolines and Saturated Aza-Heterocycles by RhI. *Angew. Chem., Int. Ed.* **2018**, *57*, 9950−9954.

(9) Roque, J. B.; Kuroda, Y.; Jurczyk, J.; Xu, L.-P.; Ham, J. S.; Göttemann, L. T.; Roberts, C. A.; Adpressa, D.; Saurí, J.; Joyce, L. A.; Musaev, D. G.; Yeung, C. S.; Sarpong, R. C−C cleavage approach to C−H functionalization of saturated aza-cycles. *ACS Catal.* **2020**, *10*, 2929−2941.

(10) Topczewski, J. J.; Cabrera, P. J.; Saper, N. I.; Sanford, M. S. Palladium-catalysed transannular C−H functionalization of alicyclic amines. *Nature* **2016**, *531*, 220−224.

(11) (a) Old, D. W.; Wolfe, J. P.; Buchwald, S. L. A highly active catalyst for palladium-catalyzed cross-coupling reactions: Room-temperature Suzuki couplings and amination of unactivated aryl chlorides. *J. Am. Chem. Soc.* **1998**, *120*, 9722−9723. (b) Surry, D. S.; Buchwald, S. L. Dialkylbiaryl phosphines in Pd-catalyzed amination: a user's guide. *Chem. Sci.* **2011**, *2*, 27−50. (c) Surry, D. S.; Buchwald, S. L. Biaryl phosphane ligands in palladium-catalyzed amination. *Angew. Chem., Int. Ed.* **2008**, *47*, 6338−6361.

(12) Recently, Sarpong and co-workers also extended this strategy to the synthesis of substituted indolizidines using a Rh complex that possesses a bidentate XantPhos ligand. See: Ham, J. S.; Park, B.; Son, M.; Roque, J. B.; Jurczyk, J.; Yeung, C. S.; Baik, M.-H.; Sarpong, R. C−H/C−C functionalization approach to N-fused heterocycles from saturated azacycles. *J. Am. Chem. Soc.* **2020**, *142*, 13041−13050.

(13) (a) Ingoglia, B. T.; Wagen, C. C.; Buchwald, S. L. Biaryl monophosphine ligands in palladium-catalyzed C−N coupling: An updated User's guide. *Tetrahedron* **2019**, *75*, 4199−4211. (b) Barder, T. E.; Biscoe, M. R.; Buchwald, S. L. Structural insights into active catalyst structures and oxidative addition to (biaryl)phosphine−palladium complexes via density functional theory and experimental studies. *Organometallics* **2007**, *26*, 2183−2192. (c) Bruno, N. C.; Tudge, M. T.; Buchwald, S. L. Design and preparation of new palladium precatalysts for C-C and C-N cross-coupling reactions. *Chem. Sci.* **2013**, *4*, 916−920. (d) Arrechea, P. L.; Buchwald, S. L. Biaryl phosphine based Pd(II) amido complexes: The effect of ligand structure on reductive elimination. *J. Am. Chem. Soc.* **2016**, *138*, 12486−12493.

(14) (a) Maimone, T. J.; Milner, P. J.; Kinzel, T.; Zhang, Y.; Takase, M. K.; Buchwald, S. L. Evidence for in Situ Catalyst Modification during the Pd-Catalyzed Conversion of Aryl Triflates to Aryl Fluorides. *J. Am. Chem. Soc.* **2011**, *133*, 18106−18109. (b) Milner, P. J.; Maimone, T. J.; Su, M.; Chen, J.; Müller, P.; Buchwald, S. L. Investigating the dearomative rearrangement of biaryl phosphine-ligated Pd(II) complexes. *J. Am. Chem. Soc.* **2012**, *134*, 19922−19934.

(15) Frisch, M. J. et al. *Gaussian 16*, rev. C.01; Gaussian, Inc.: Wallingford, CT, 2016. (See the SI for the full citation.)

(16) (a) Hay, P. J.; Wadt, W. R. Ab initio effective core potentials for molecular calculations. Potentials for K to Au including the outermost core orbitals. *J. Chem. Phys.* **1985**, *82*, 299−310. (b) Wadt, W. R.; Hay, P. J. Ab initio effective core potentials for molecular calculations. Potentials for main group elements Na to Bi. *J. Chem. Phys.* **1985**, *82*, 284−298.

(17) (a) Becke, A. D. Density-functional exchange-energy approximation with correct asymptotic behavior. *Phys. Rev. A: At., Mol., Opt. Phys.* **1988**, *38*, 3098−3100. (b) Lee, C.; Yang, W.; Parr, R. G. Development of the Colle-Salvetti correlation-energy formula into

a functional of the electron density. *Phys. Rev. B: Condens. Matter Mater. Phys.* **1988**, *37*, 785−789. (c) Becke, A. D. A new mixing of Hartree−Fock and local density-functional theories. *J. Chem. Phys.* **1993**, *98*, 1372−1377.
(18) (a) Grimme, S.; Antony, J.; Ehrlich, S.; Krieg, H. A consistent and accurate ab initio parametrization of density functional dispersion correction (DFT-D) for the 94 elements H-Pu. *J. Chem. Phys.* **2010**, *132*, 154104. (b) Grimme, S.; Hansen, A.; Brandenburg, J. G.; Bannwarth, C. Dispersion-corrected mean-field electronic structure methods. *Chem. Rev.* **2016**, *116*, 5105−5154.
(19) Becke, A. D.; Johnson, E. R. Exchange-hole dipole moment and the dispersion interaction. *J. Chem. Phys.* **2005**, *122*, 154104.
(20) Cancès, E.; Mennucci, B.; Tomasi, J. A new integral equation formalism for the polarizable continuum model: Theoretical background and applications to isotropic and anisotropic dielectrics. *J. Chem. Phys.* **1997**, *107*, 3032−3041.
(21) Küchle, W.; Dolg, M.; Stoll, H.; Preuss, H. Energy-adjusted pseudopotentials for the actinides. Parameter sets and test calculations for thorium and thorium monoxide. *J. Chem. Phys.* **1994**, *100*, 7535−7542.
(22) Legault, C. Y. *CYLview, 1.0b*; Université de Sherbrooke, 2009. http://www.cylview.org.
(23) Johnson, E. R.; Keinan, S.; Mori-Sánchez, P.; Contreras-García, J.; Cohen, A. J.; Yang, W. Revealing noncovalent interactions. *J. Am. Chem. Soc.* **2010**, *132*, 6498−6506.
(24) Lu, T.; Chen, F. Multiwfn: A multifunctional wavefunction analyzer. *J. Comput. Chem.* **2012**, *33*, 580−592.
(25) Humphrey, W.; Dalke, A.; Schulten, K. VMD - visual molecular dynamics. *J. Mol. Graphics* **1996**, *14*, 33−38.
(26) In our calculations, we assumed the Cs_2CO_3 molecule as a model of the Cs_2CO_3 salt utilized in the experiments because in the reported experiments we had used a large amount of base (1.2 equiv, which is 48 times large than the used Pd), and reaction time was 24h. It can be expected that the utilized reaction condition, as well as the presence of the carbonyl and hydroxyl groups in the used substrate *N*-Fused Bicyclo *α*-Hydroxy-*β*-Lactam, would improve solubility of the Cs-carbonate and make available of the molecular Cs_2CO_3. Regardless, we have also validated the presence of small Cs_2CO_3-clusters in the reaction mixture, and have studied stability of the Cs_2CO_3-dimer and Cs_2CO_3-tetramer (see the Supporting Information for more details).
(27) The formation of **2** might be a multistep process which can involve a series of "two-component" and/or "three-component" reactions. We have calculated the free energies for a series of such reactions which are presented in the Supporting Information (see section 1, eqs 1−6). These reactions are directly related to the formation of species **2**, which is formed in a sequence of steps and not through a single collision event to bring together all the components. We found that the formation of intermediate **2** is highly exergonic (by 32.7 kcal/mol). Therefore, we considered **2** as the reaction starting material en route to the oxidative addition step.
(28) Xu, L.-P.; Haines, B. E.; Ajitha, M. J.; Murakami, K.; Itami, K.; Musaev, D. G. Roles of base in the Pd-catalyzed annulative chlorophenylene Dimerization. *ACS Catal.* **2020**, *10*, 3059−3073.
(29) Li, B.-W.; Wang, M.-Y.; Fang, S.; Liu, J.-Y. DFT study on the mechanism of Palladium(0)-catalyzed reaction of aryl iodides, norbornene, and di-tert-butyldiaziridinone. *Organometallics* **2019**, *38*, 2189−2198.
(30) In **TS-1oa**, one of the Cs-cations (Cs^1) interacts with the incoming Br-anion. As a result, the rest of the base, i.e., the [$CsCO_3$]-unit, is rendered a partially anionic character and abstracts the proton from the neighboring (located within H-bonding distance) *α*-hydroxy-*β*-lactam. The calculated H−O^4(lactam) = 1.445 Å and H−O^3(carbonate) = 1.058 Å, in the TS. In the product (**3**), the Br-anion has transferred to the Cs-cation and not the Pd-center. Therefore, one of the O atoms of the [$CsCO_3$] anion has to interact with the coordinately unsaturated Pd-center to complete the "oxidative addition" process. This results in a proton release from the [$CsCO_3$] moiety, which returns to the lactam before the O−Pd bond formation. The calculated H^1−O^3 = 1.413 Å and (H^1−O^4: 1.057 Å) in the product.
(31) McLarney, B. D.; Hanna, S.; Musaev, D. G.; France, S. Predictive model for the [Rh_2(esp)$_2$]-catalyzed intermolecular C(sp^3)−H bond insertion of *β*-carbonyl ester carbenes: interplay between theory and experiment. *ACS Catal.* **2019**, *9*, 4526−4538.
(32) Park, Y.; Chang, S. Asymmetric formation of *γ*-lactams via C−H amidation enabled by chiral hydrogen-bond-donor catalysts. *Nat. Catal.* **2019**, *2*, 219−227.
(33) The large exergonicity of the Ph−Br oxidative addition reaction in the presence of base is due to the formation of strong Pd−O (carbonate) and Cs−Br bonds, along with the Pd−C bond, during this process.
(34) The increase of activation barrier in the presence of Cs_2CO_3 is due to increase of steric hindrance around the Pd-center that reduces accessibility of the Pd-center. In the meantime, the presence of the base increases exergonicity of the oxidative addition reaction because of formation of the strong Pd−O (carbonate) and Cs−Br bonds, along with the Pd−C bond, during the process.
(35) Musaev, D. G.; Figg, T. M.; Kaledin, A. L. Versatile reactivity of Pd-catalysts: mechanistic features of the mono-N-protected amino acid ligand and cesium-halide base in Pd-catalyzed C−H bond functionalization. *Chem. Soc. Rev.* **2014**, *43*, 5009−5031.
(36) Previously (see ref 9), we have discussed the PES of the reactions initiated from Pd-alcoholates **6** at the B3LYP-D3(BJ)/BS1 + (IEF-PCM) level of theory. Here, we apply a better level of theory, [B3LYP-D3(BJ)/BS2 + (IEF-PCM)]//[B3LYP-D3BJ/BS1 + (IEF-PCM)]. In general, slight changes in the absolute energy values using this higher level of theory did not change the conclusions we reached previously.
(37) As we have previously shown (see ref 9), the Pd-alcoholate intermediate may possess several isomeric forms. In Figure 3, we depict its energetically most favorable (k^2-O,O) isomer, **6**, where the *β*-lactam is coordinated to the Pd(II)-center via the carbonyl and hydroxy oxygens. Alternatively, a κ^2-O,H isomer, **6a**, where the *β*-lactam moiety is coordinated to the Pd(II)-center via the tertiary alcohol group and hydrogen at C^p, may form (see Figure S4 in Supporting Information). Calculations showed that isomer **6** is 4.0 kcal/mol favorable than **6a**. These two isomers of the Pd-alcoholate interconvert through a small energy barrier.
(38) (a) Alabugin, I. V. *Stereoelectronic effects: A bridge between structure and reactivity*; John Wiley & Sons: Chichester, 2016. (b) Alabugin, I. V.; dos Passos Gomes, G.; Abdo, M. A. Hyperconjugation. *Wiley Interdiscip. Rev.: Comput. Mol. Sci.* **2019**, *9*, e1389. (c) Alabugin, I. V.; Zeidan, T. A. Stereoelectronic effects and general trends in hyperconjugative acceptor ability of *σ* bonds. *J. Am. Chem. Soc.* **2002**, *124*, 3175−3185.
(39) (a) Ess, D. H.; Houk, K. N. Distortion/interaction energy control of 1,3-dipolar cycloaddition reactivity. *J. Am. Chem. Soc.* **2007**, *129*, 10646−10647. (b) Bickelhaupt, F. M.; Houk, K. N. Analyzing reaction rates with the distortion/interaction-activation strain model. *Angew. Chem., Int. Ed.* **2017**, *56*, 10070−10086. (c) dos Passos Gomes, G.; Alabugin, I. V. Drawing catalytic power from charge separation: Stereoelectronic and zwitterionic assistance in the Au(I)-catalyzed Bergman cyclization. *J. Am. Chem. Soc.* **2017**, *139*, 3406−3416.
(40) (a) Glendening, E. D.; Streitwieser, A. Natural energy decomposition analysis: An energy partitioning procedure for molecular interactions with application to weak hydrogen bonding, strong ionic, and moderate donor−acceptor interactions. *J. Chem. Phys.* **1994**, *100*, 2900−2909. (b) Glendening, E. D. Natural energy decomposition analysis: Extension to density functional methods and analysis of cooperative effects in water clusters. *J. Phys. Chem. A* **2005**, *109*, 11936−11940. (c) Glendening, E. D. Natural energy decomposition analysis: Explicit evaluation of electrostatic and polarization effects with application to aqueous clusters of alkali metal cations and neutrals. *J. Am. Chem. Soc.* **1996**, *118*, 2473−2482. For a recent example of energy decomposition analysis, see: (d) Qi, X.; Kohler, D. G.; Hull, K. L.; Liu, P. Energy decomposition analyses

https://dx.doi.org/10.1021/jacs.0c10220
J. Am. Chem. Soc. 2020, 142, 21140−21152

reveal the origins of catalyst and nucleophile effects on regioselectivity in nucleopalladation of alkenes. *J. Am. Chem. Soc.* **2019**, *141*, 11892−11904.
(41) We also used the NBODEL approach to calculate the Pd−O/C^2 donor−acceptor interactions. The results of these new sets of calculations are fully consistent with our present NBO calculations. Especially, the difference in the calculated interaction energies ($\Delta E(2)$) between **TS-6p** and **TS-6d** remains the same with both NBODEL and NBO calculations (see the Supporting Information for details).
(42) It should be noted that we have searched several important conformations for each reported structures based on the aforementioned possible binding modes (i.e., "C-bound" or "O-bound," Scheme 3) of the Buchwald's type of ligand and the most stable ones are discussed here (for others, see the Supporting Information).
(43) We have calculated the transition state and products of the C−H bond activation in $-OCF_2H$ substituent by the Pd-carbonate. The calculated 46.7 kcal/mol free energy barrier for this process is very high for it to be practical. Therefore, this pathway can be safely excluded from discussion (see the Supporting Information for more details).
(44) Vatsadze, S. Z.; Loginova, Y. D.; dos Passos Gomes, G.; Alabugin, I. V. Stereoelectronic chameleons: The donor-acceptor dichotomy of functional groups. *Chem. - Eur. J.* **2017**, *23*, 3225−3245.
(45) Larini, P.; Kefalidis, C. E.; Jazzar, R.; Renaudat, A.; Clot, E.; Baudoin, O. On the mechanism of the palladium-catalyzed β-arylation of ester enolates. *Chem. - Eur. J.* **2012**, *18*, 1932−1944.
(46) For the β-arylation and vinylation reactions, the rate-limiting transition states are the alkene reinsertion TSs. For the sake of simplicity of our analyses, here, we accepted the transition states β-RE to be the β-selective arylation and vinylation controlling one, too. This assumption is not going to impact our final conclusions. (For details on the comparison between α-RE and reinsertion with aryl and alkynyl substrates, see the Supporting Information).
(47) Culkin, D. A.; Hartwig, J. F. Carbon−carbon bond-forming reductive elimination from arylpalladium complexes containing functionalized alkyl groups. Influence of ligand steric and electronic properties on structure, stability, and reactivity. *Organometallics* **2004**, *23*, 3398−3416.

https://dx.doi.org/10.1021/jacs.0c10220
J. Am. Chem. Soc. 2020, 142, 21140−21152